Rotating mistuned bladed disk assembly dynamic response prediction using component mode synthesis methods with interface modes

F. Duvauchelle, Duc-Minh Tran, Roger Ohayon

▶ **To cite this version:**

F. Duvauchelle, Duc-Minh Tran, Roger Ohayon. Rotating mistuned bladed disk assembly dynamic response prediction using component mode synthesis methods with interface modes. ASME 2005 International Design Engineering Technical Conferences, IDETC 2005, Sep 2005, Long Beach, United States. ⟨10.1115/DETC2005-85216⟩. ⟨hal-03179544⟩

HAL Id: hal-03179544

https://hal.science/hal-03179544v1

Submitted on 29 Feb 2024

HAL is a multi-disciplinary open access archive for the deposit and dissemination of scientific research documents, whether they are published or not. The documents may come from teaching and research institutions in France or abroad, or from public or private research centers.

L'archive ouverte pluridisciplinaire **HAL**, est destinée au dépôt et à la diffusion de documents scientifiques de niveau recherche, publiés ou non, émanant des établissements d'enseignement et de recherche français ou étrangers, des laboratoires publics ou privés.

HAL Authorization

ROTATING MISTUNED BLADED DISK ASSEMBLY DYNAMIC RESPONSE PREDICTION USING COMPONENT MODE SYNTHESIS METHODS WITH INTERFACE MODES

Francois Duvauchelle
ONERA
Structural Dynamics
and Coupled Systems Department
BP 72, Châtillon, F-92322, France
Email: francois.duvauchelle@onera.fr

Duc-Minh Tran
ONERA
Structural Dynamics
and Coupled Systems Department
BP 72, Châtillon, F-92322, France
Email: minh.tran_duc@onera.fr

Roger Ohayon
CNAM
Structural Mechanics
and Coupled Systems Laboratory
2 rue Conté, Paris, F-75003, France
Email: ohayon@cnam.fr

ABSTRACT

Finite element-based reduced order methods are presented with application to the prediction of rotating mistuned bladed disk forced response. These methods have already been applied to tuned non-rotating models having cyclic symmetry. The aim is to reduce significantly the number of interface co-ordinates, which can be very important in classical component mode synthesis methods. The approach is based on the use of the interface modes which result from a static condensation of the whole structure on the whole interface. A first implementation of this procedure and numerical results are presented.

INTRODUCTION

Turbomachine blades are very sensitive to small variations on blade to blade properties. These variations, called mistuning, result from manufacturing tolerances or inner deviations of material properties, and may appear randomly around all the bladed-disk assemblies. The presence of mistuning has significant consequences on the behaviour of the entire structure. One particular consequence is the apparition of a severe mode localisation phenomenon [1–3], but it would also has a beneficial stabilizing effect in a flutter situation [4, 5].

A widely used approach to study mistuned models consists in finite element-based reduced order methods. As an advantage, they are very appropriated to calculate the response of a structure with acceptable computational costs, and they can capture the true behavior of a real mistuned bladed disk, contrary to the simple analytical models used before.

We can separate these latest methods in two groups. The first group contains all methods based on the use of a subset of nominal modes [6, 7], while the second group gathers methods based on component mode synthesis (CMS) [7, 8]. The study presented in this paper is in this last line.

All CMS methods aim at performing the dynamic analysis of structures by breaking them into substructures. Then, these substructures, also named components, are represented by their modes (in the sense of Ritz vectors), which contains the vibration normal modes, the static modes, the interface modes, etc. Depending on the nature of the interface, four large groups of methods have been developped: fixed interface [9, 10], free interface [11, 12], hybrid interface [13] and loaded interface methods [14], and the coupling of the differents substructures is generaly performed through the interface displacements.

As part of the tuned structure analysis, Henry [15] combined the cyclic symmetry reduction [16] with Craig and Bampton's method, and shown the efficiency of this procedure. In most of the real industrial structures, the problem is that the classical CMS methods lead to a great number of degrees of freedom at the interface. So, in order to reduce the number of interface co-ordinates and therefore, the size of the coupled system, Bourquin [17, 18] described a reduction procedure for the fixed

interface CMS method based on the use of the interface modes. Tran [19] generalized this procedure in the cases of free and hybrid interface CMS methods, with application to structures having a cyclic symmetry. For each CMS method, the idea consists in introducing the interface modes in place of the static modes in the set of Ritz vectors on which the structure motion equation is projected.

In this article, the reduction procedures proposed by Bourquin and Tran are extended in the case of rotating mistuned bladed-disk assemblies. In a first part, the motion equation of rotating structures is reminded with its properties. Then, the model description is presented, in both tuned and mistuned cases, before introducing the formulations of classical component mode synthesis methods, and these using the interface modes. Finally, the procedure based on the use of the interface modes and numerical simulation obtained on a simplified development model are presented.

EQUATION OF ROTATING STRUCTURES

The discretized equilibrium equation of a rotating bladed disk assembly S is written as :

$$\mathbf{M}^S\ddot{\mathbf{x}}^S + [\mathbf{C}^S + \mathbf{G}^S]\dot{\mathbf{x}}^S + [\mathbf{K}_{\mathrm{E}}^S + \mathbf{K}_{\mathrm{S}}^S + \mathbf{K}_{\mathrm{G}}^S + \mathbf{K}_{\mathrm{A}}^S]\mathbf{x}^S = \mathbf{f}^S(\mathbf{x}^S, \dot{\mathbf{x}}^S), \tag{1}$$

with $\mathbf{M}^S$, $\mathbf{K}_{\mathrm{E}}^S$, and $\mathbf{C}^S$ are the mass, elastic stiffness, and damping matrices of S, $\mathbf{G}^S$ is the gyroscopic (Coriolis) matrix. The gyroscopic effect implies a coupling between the displacements normal to the rotation axis, which has an important role in the behaviour of rotating shaft, but can generally be neglected in case of bladed disks. $\mathbf{K}_{\mathrm{S}}^S$ contains the spin softening effects, which takes geometry variations into account. In our particular case which consists in a rotation arround the rotational axis with a cylindrical reference frame, it can be shown that $\mathbf{K}_{\mathrm{S}}^S = -\Omega^2\mathbf{M}^S$, where Ω is the instantaneous rotational speed of the structure arround its axis. $\mathbf{K}_{\mathrm{G}}^S$ represent the centrifugal stress stiffening. This nonlinear effect couples the in-plane and transverse displacements, and would be very important in case of thin structures with small bending stiffness compared to axial stiffness. Finally, $\mathbf{K}_{\mathrm{A}}^S$ depends on the derivative of the rotational speed, and would have an important effect on the maximum deflection of the structure displacements when rotational speed increases. In the following, we will consider a constant rotational speed, so that $\mathbf{K}_{\mathrm{A}}^S$ will be null. $\mathbf{x}^S$ is the vector of physical co-ordinates of S, and finaly $\mathbf{f}^S(\mathbf{x}^S, \dot{\mathbf{x}}^S)$ is the vector of external forces applied to S. The matrices $\mathbf{M}^S$, $\mathbf{K}_{\mathrm{E}}^S$ and $-\mathbf{K}_{\mathrm{S}}^S$ are symmetric and positive definite, whereas $\mathbf{G}^S$ is an anti-symmetric positive definite matrix. Note that the case of rotor blade is not considered in the following.

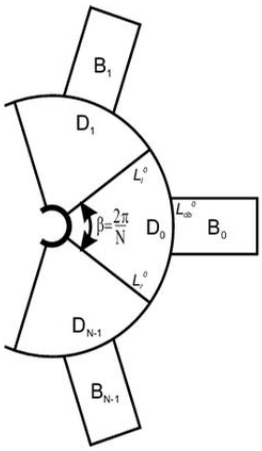

Figure 1. STRUCTURAL NOTATIONS.

DESCRIPTION OF THE BLADED DISK MODEL

We consider a rotating structure S decomposed into N sectors S_j which do not overlap as represented on Fig. 1. Each sector S_j, $j = 0,...,N-1$, is made up of a blade B_j and a part of disk D_j. We denote by L, the part of S which constitutes the interface between all substructures B_j and D_j. L^{D_j} is the part of L associated with the substructure D_j, such as $L^{D_j} = L_{\mathrm{r}}^{D_j} \cup L_{\mathrm{l}}^{D_j} \cup L_{\mathrm{b}}^{D_j}$, with $L_{\mathrm{r}}^{D_j}$ and $L_{\mathrm{l}}^{D_j}$, the right and left boundaries of D_j, and $L_{\mathrm{b}}^{D_j}$, the boundary between D_j and B_j. The blade B_j is associated with $L^{B_j} = L_{\mathrm{b}}^{D_j}$. In the following developments, the reference sector, blade, or part of disk, will be denoted by the subscript or superscript 0.

Cyclic symmetry model

In the tuned case, we consider the structure S which consists in N sectors S_0,...,S_{N-1}, identical by a rotation of $\beta = 2\pi/N$ around the rotation axis $(O, \overrightarrow{z})$ in the cylindrical reference system (r, θ, z). Note that there is no need to distinguish D_j and B_j in this tuned model.

The cyclic symmetry assumption and the boundary conditions allow the discretisation and the reduction of the study to the reference sector S_0, which leads to N systems of motion equations :

$$\begin{cases} \mathbf{M}^{S_0}\ddot{\mathbf{u}}_n + \mathbf{B}^{S_0}\dot{\mathbf{u}}_n + \mathbf{K}^{S_0}\mathbf{u}_n = \mathbf{f}_n + \mathbf{r}_n \\ \mathbf{u}_{n_{L_{\mathrm{l}}^{S_0}}} = \mathbf{u}_{n_{L_{\mathrm{r}}^{S_0}}} \mathrm{e}^{\mathrm{i}\sigma_n} \end{cases}, \tag{2}$$

where $\mathbf{B}^{S_0} = \mathbf{C}^{S_0} + \mathbf{G}^{S_0}$, $\mathbf{K}^{S_0} = \mathbf{K}_{\mathrm{E}}^{S_0} + \mathbf{K}_{\mathrm{S}}^{S_0} + \mathbf{K}_{\mathrm{G}}^{S_0}$, $\mathbf{u}_n = \mathbf{u}_n(S_0, t)$ is the vector of travelling wave co-ordinates of the sector S_0, $\sigma_n = n\beta$ is the phase angle associated with the phase number n. $L_{\mathrm{l}}^{S_0}$ and $L_{\mathrm{r}}^{S_0}$ reference the left and right boundaries of S_0. Last,

$\mathbf{f}_n = \frac{1}{N}\sum_{k=0}^{N-1} \mathbf{f}^{S_k}\, \mathrm{e}^{-\mathrm{i}k\sigma_n}$, where $\mathbf{f}^{S_k}$ represent the external forces applied to S_k and $\mathbf{r}_n$ are the reactions at the boundaries of S_0 and its adjacent sectors.

The vector of real physical displacements of S_k, for $k = 0,...,N-1$, is obtained from the travelling waves co-ordinates $\mathbf{u}_n$ as follows :

$$\mathbf{U}(S_k,t) = \Re\left\{\sum_{n=0}^{N-1} \mathbf{u}_n \mathrm{e}^{\mathrm{i}k\sigma_n}\right\}. \tag{3}$$

Mistuned model

In order to represent most of real cases, each sector S_j, $j = 0,...,N-1$, is subdivided in two substructures B_j and D_j associated with a blade and a part of the disk. Thus, two configurations are envisaged :

- tuned disk and mistuned blades ;
- mistuned disk and mistuned blades.

In the following, we will now denote by S_j the substructure D_j or B_j. The approach adopted in this work to take mistuning into account consists in adding perturbation matrices to the mass and stiffness matrices. In this way, the mistuning pattern is described as follows :

$$\mathbf{M}^{S_j}_{\text{mistuned}} = \mathbf{M}^{S_j}_{\text{tuned}} + \Delta\mathbf{M}^{S_j}, \tag{4}$$
$$\mathbf{K}^{S_j}_{\text{mistuned}} = \mathbf{K}^{S_j}_{\text{tuned}} + \Delta\mathbf{K}^{S_j}, \tag{5}$$

with S_j tuned mass and stiffness matrices $\mathbf{M}^{S_j}_{\text{tuned}}$ and $\mathbf{K}^{S_j}_{\text{tuned}}$, and their perturbation matrices $\Delta\mathbf{M}^{S_j}$ and $\Delta\mathbf{K}^{S_j}$. These matrices $\Delta\mathbf{M}^{S_j}$ and $\Delta\mathbf{K}^{S_j}$ can be generated by Monte Carlo's simulations, but they could also be obtained by a deterministic manner in the view to study a few particular mistuning patterns (perturbation on the blades length, on their Young's moduli, or geometric perturbation directly in the structural finite element model). In the case of random perturbations, matrices $\Delta\mathbf{M}^{S_j}$ and $\Delta\mathbf{K}^{S_j}$ are generated in such a way that their infinte norms are less than scalar factors $\varepsilon_{\mathbf{M}^{S_j}}$ and $\varepsilon_{\mathbf{K}^{S_j}}$:

$$\|\Delta\mathbf{M}^{S_j}\|_\infty \leqslant \varepsilon_{\mathbf{M}^{S_j}} \text{ and } \|\Delta\mathbf{K}^{S_j}\|_\infty \leqslant \varepsilon_{\mathbf{K}^{S_j}}. \tag{6}$$

The structural damping is supposed to verify the Rayleigh's assumption. So the damping matrices $\mathbf{C}^{S_j}$ are assumed to be proportional to the mass and stiffness matrices of S_j such as : $\mathbf{C}^{S_j} = \alpha\mathbf{M}^{S_j} + \beta\mathbf{K}^{S_j}$, with α and β, two scalar factors which depend on the model.

CLASSICAL CMS METHODS

We consider the structure as presented in Fig. 1. The interface L^{S_j} can be separated in two parts : a fixed interface $L_{\text{c}}^{S_j}$ and a free interface $L_{\text{a}}^{S_j}$. Physical co-ordinate vectors of S, L, S_j, L^{S_j}, $L_{\text{c}}^{S_j}$, and $L_{\text{a}}^{S_j}$ are respectively $\mathbf{x}^S$, $\mathbf{x}_L^S$, $\mathbf{x}^{S_j}$, $\mathbf{x}_L^{S_j}$, $\mathbf{x}_{Lc}^{S_j}$, $\mathbf{x}_{\text{La}}^{S_j}$, and their dimensions are n^S, n_L^S, n^{S_j}, $n_L^{S_j}$, $n_{Lc}^{S_j}$, and $n_{\text{La}}^{S_j}$. If substructures S_j are unconstraint and have $n_{\text{r}}^{S_j}$ rigid body modes, $n_{\text{r}}^{S_j}$ rigid body co-ordinates $\mathbf{x}_{\text{r}}^{S_j}$ are choosen among the physical co-ordinates $\mathbf{x}^{S_j}$, in order to make substructures isostatically constraint during the computation of the attachment modes, by fixing co-ordinates $\mathbf{x}_{\text{r}}^{S_j}$. Matrices $\mathbf{P}^{S_j}$, $\mathbf{P}_L^S$, $\mathbf{P}_{Lc}^{S_j}$ and $\mathbf{P}_{\text{La}}^{S_j}$ achieve the following restrictions $\mathbf{x}^{S_j} = \mathbf{P}^{S_j}\mathbf{x}^S$, $\mathbf{x}_L^S = \mathbf{P}_L^S\mathbf{x}^S$, $\mathbf{x}_{Lc}^{S_j} = \mathbf{P}_{Lc}^{S_j}\mathbf{x}^S$, and $\mathbf{x}_{\text{La}}^{S_j} = \mathbf{P}_{\text{La}}^{S_j}\mathbf{x}^S$. For each substructure S_j, the interface L^{S_j}, can b of three different types. In the fixed interface case, $n_{\text{La}}^{S_j} = 0$ and $n_{Lc}^{S_j} = n_L^{S_j}$. For a free interface, $n_{Lc}^{S_j} = 0$ and $n_{\text{La}}^{S_j} = n_L^{S_j}$, whereas an hybrid interface is distinguished by $n_{Lc}^{S_j} = 0 > 0$, $n_{\text{La}}^{S_j} > 0$ and $n_{Lc}^{S_j} + n_{\text{La}}^{S_j} = n_L^{S_j}$. In this last case, we suppose that S_j is constraint when the vector $\mathbf{x}_{Lc}^{S_j}$ is fixed.

According to Eqn. (1), the equilibrium equation of a rotating substructure S_j can be written as follows :

$$\mathbf{M}^{S_j}\ddot{\mathbf{x}}^{S_j} + \mathbf{B}^{S_j}\dot{\mathbf{x}}^{S_j} + \mathbf{K}^{S_j}\mathbf{x}^{S_j} = \mathbf{f}^{S_j} - {}^{\text{t}}\mathbf{P}_{Lc}^{S_j}\mathbf{f}_{Lc}^{S_j} - {}^{\text{t}}\mathbf{P}_{\text{La}}^{S_j}\mathbf{f}_{\text{La}}^{S_j}, \tag{7}$$

where $\mathbf{B}^{S_j} = \mathbf{C}^{S_j} + \mathbf{G}^{S_j}$, $\mathbf{K}^{S_j} = \mathbf{K}_{\text{E}}^{S_j} + \mathbf{K}_{\text{S}}^{S_j} + \mathbf{K}_{\text{G}}^{S_j}$, $\mathbf{f}^{S_j}$ is the vector of external forces applied to S_j, $\mathbf{f}_{Lc}^{S_j}$ and $\mathbf{f}_{\text{La}}^{S_j}$ are the interface reactions applied to $L_{\text{c}}^{S_j}$ and $L_{\text{a}}^{S_j}$. The physical displacements o the substructure S_j are formulated as a linear combination of the substructure normal modes, rigid body modes and static modes. Then, few transformations lead to a set of Ritz vectors $\mathbf{Q}^{S_j}$ such as :

$$\mathbf{x}^{S_j} = \mathbf{Q}^{S_j}\left\{\begin{array}{c}\boldsymbol{\mu}^{S_j}\\ \mathbf{x}_L^{S_j}\end{array}\right\}, \tag{8}$$

with $\boldsymbol{\mu}^{S_j}$, the generalized co-ordinates, $\mathbf{x}_L^{S_j}$, the interface displacements, and $\mathbf{Q}^{S_j}$, a set of Ritz vectors whose expression come from the choosen component mode synthesis method. By projecting the motion equation (7) on the set of Ritz vectors $\mathbf{Q}^{S_j}$, we obtain the reduced system :

$$\begin{aligned}{}^{\text{t}}\mathbf{Q}^{S_j}\mathbf{M}^{S_j}\mathbf{Q}^{S_j}\left\{\begin{array}{c}\ddot{\boldsymbol{\mu}}^{S_j}\\ \ddot{\mathbf{x}}_L^{S_j}\end{array}\right\} + {}^{\text{t}}\mathbf{Q}^{S_j}\mathbf{B}^{S_j}\mathbf{Q}^{S_j}\left\{\begin{array}{c}\dot{\boldsymbol{\mu}}^{S_j}\\ \dot{\mathbf{x}}_L^{S_j}\end{array}\right\}\\ + {}^{\text{t}}\mathbf{Q}^{S_j}\mathbf{K}^{S_j}\mathbf{Q}^{S_j}\left\{\begin{array}{c}\boldsymbol{\mu}^{S_j}\\ \mathbf{x}_L^{S_j}\end{array}\right\} = {}^{\text{t}}\mathbf{Q}^{S_j}\mathbf{f}^{S_j} - \left\{\begin{array}{c}0\\ \mathbf{f}_L^{S_j}\end{array}\right\}.\end{aligned} \tag{9}$$

The interface continuity and the force equilibrium on the boundaries allow to achieve the coupling between all different substructures S_j. As a consequence, the solutions of the coupled system provide the generalized co-ordinates $\boldsymbol{\mu}^{S_j}$, and the $n_L^{S_j}$ interface displacements $\mathbf{x}_L^{S_j}$. Physical displacements $\mathbf{x}^{S_j}$ of each substructure S_j are then obtained by using Eqn. (8).

The different component mode synthesis methods refer to the following modes :

- the first m^{S_j} normal modes $\boldsymbol{\Phi}^{S_j}$ of the undamped substructure S_j, with fixed, free or hybrid interface ;
- the $n_{\mathrm{r}}^{S_j}$ rigid body modes $\boldsymbol{\Psi}_{\mathrm{r}}^{S_j}$ in the case of unconstraint substructures with free interface ;
- the $n_L^{S_j}$ constraint modes $\boldsymbol{\Psi}_C^{S_j}$ associated with the interface L^{S_j}. They are obtained by enforcing successively a unit displacement on each co-ordinate of L^{S_j}, while fixing all others co-ordinates of L^{S_j}. The constraint modes $\boldsymbol{\Psi}_C^{S_j}$ are subdivided in two sets of modes : $\boldsymbol{\Psi}_{C\mathrm{c}}^{S_j}$ and $\boldsymbol{\Psi}_{C\mathrm{a}}^{S_j}$, corresponding respectively to the unit displacements imposed on $L_{\mathrm{c}}^{S_j}$ and $L_{\mathrm{a}}^{S_j}$;
- the $n_{L\mathrm{c}}^{S_j}$ constraint modes $\boldsymbol{\Psi}_{\mathrm{c}}^{S_j}$ associated with the interface $L_{\mathrm{c}}^{S_j}$. These modes are only defined in the case of hybrid interface and they are obtained similarly as the modes $\boldsymbol{\Psi}_C^{S_j}$, with the particular difference that $L_{\mathrm{a}}^{S_j}$ remains free. The constraint modes $\boldsymbol{\Psi}_{\mathrm{c}}^{S_j}$ verify the expression :

$$\boldsymbol{\Psi}_{\mathrm{c}}^{S_j} = \boldsymbol{\Psi}_{C\mathrm{c}}^{S_j} + \boldsymbol{\Psi}_{C\mathrm{a}}^{S_j\,\mathrm{a}}\boldsymbol{\Psi}_{\mathrm{c}}^{S_j}\,, \tag{10}$$

  where ${}^{\mathrm{a}}()$ designate the restriction to the interface $L_{\mathrm{a}}^{S_j}$;
- the $n_{L\mathrm{a}}^{S_j}$ attachment modes $\boldsymbol{\Psi}_{\mathrm{a}}^{S_j}$ of $L_{\mathrm{a}}^{S_j}$ and obtained by applying on each co-ordinate of $L_{\mathrm{a}}^{S_j}$ the opposite of a unit force, keeping $L_{\mathrm{c}}^{S_j}$ fixed ;
- the $n_{L\mathrm{a}}^{S_j}$ residual attachment modes $\boldsymbol{\Psi}_{\mathrm{ar}}^{S_j}$ obtained by removing the contribution of the undamped normal modes $\boldsymbol{\Phi}^{S_j}$ already contained in $\boldsymbol{\Psi}_{\mathrm{a}}^{S_j}$;
- the $n_{L\mathrm{a}}^{S_j}$ normalized attachment modes and residual attachment modes $\boldsymbol{\Psi}_{\mathrm{a}}^{\prime S_j}$ and $\boldsymbol{\Psi}_{\mathrm{ar}}^{\prime S_j}$ whose expressions are :

$$\boldsymbol{\Psi}_{\mathrm{a}}^{\prime S_j} = \boldsymbol{\Psi}_{\mathrm{a}}^{S_j}({}^{\mathrm{a}}\boldsymbol{\Psi}_{\mathrm{a}}^{S_j})^{-1} \text{ and } \boldsymbol{\Psi}_{\mathrm{ar}}^{\prime S_j} = \boldsymbol{\Psi}_{\mathrm{ar}}^{S_j}({}^{\mathrm{a}}\boldsymbol{\Psi}_{\mathrm{ar}}^{S_j})^{-1}. \tag{11}$$

The formulations of the five component mode synthesis methods presented below are based on Eqn. (8), and their differences appear only in the expressions of the physical displacements and of the matrices of Ritz vectors $\mathbf{Q}^{S_j}$.

Thus, in the fixed interface method cases, Eqn. (8) gives :

$$\mathbf{x}^{S_j} = \boldsymbol{\Phi}^{S_j}\boldsymbol{\mu}^{S_j} + \boldsymbol{\Psi}_C^{S_j}\mathbf{x}_L^{S_j}\,, \tag{12}$$

$$\mathbf{Q}^{S_j} = [\boldsymbol{\Phi}^{S_j}, \boldsymbol{\Psi}_C^{S_j}]. \tag{13}$$

In the same way, Tran [19] has shown that for the free interface methods with attachment modes, the displacements vector, and as a consequence, the matrix $\mathbf{Q}^{S_j}$ can be written as :

$$\begin{aligned}\mathbf{x}^{S_j} &= \boldsymbol{\Phi}^{S_j}\boldsymbol{\mu}^{S_j} + \boldsymbol{\Psi}_{\mathrm{r}}^{S_j}\boldsymbol{\xi}_{\mathrm{r}}^{S_j} + \boldsymbol{\Psi}_{\mathrm{a}}^{S_j}\boldsymbol{\xi}_{\mathrm{a}}^{S_j}\\ &= (\boldsymbol{\Phi}^{S_j} - \boldsymbol{\Psi}_{\mathrm{a}}^{\prime S_j\,\mathrm{a}}\boldsymbol{\Phi}^{S_j})\boldsymbol{\mu}^{S_j} + (\boldsymbol{\Psi}_{\mathrm{r}}^{S_j} - \boldsymbol{\Psi}_{\mathrm{a}}^{\prime S_j\,\mathrm{a}}\boldsymbol{\Psi}_{\mathrm{r}}^{S_j})\boldsymbol{\xi}_{\mathrm{r}}^{S_j}\\ &\quad + \boldsymbol{\Psi}_{\mathrm{a}}^{\prime S_j}\mathbf{x}_L^{S_j}\,, \end{aligned}\tag{14}$$

$$\mathbf{Q}^{S_j} = [\boldsymbol{\Phi}^{S_j} - \boldsymbol{\Psi}_{\mathrm{a}}^{\prime S_j\,\mathrm{a}}\boldsymbol{\Phi}^{S_j}, \boldsymbol{\Psi}_{\mathrm{r}}^{S_j} - \boldsymbol{\Psi}_{\mathrm{a}}^{\prime S_j\,\mathrm{a}}\boldsymbol{\Psi}_{\mathrm{r}}^{S_j}, \boldsymbol{\Psi}_{\mathrm{a}}^{\prime S_j}], \tag{15}$$

with respectively $\boldsymbol{\xi}_{\mathrm{r}}^{S_j}$ and $\boldsymbol{\xi}_{\mathrm{a}}^{S_j}$, the generalized co-ordinates associated with the rigid body modes and the attachment modes. Using the residual attachment modes :

$$\begin{aligned}\mathbf{x}^{S_j} &= \boldsymbol{\Phi}^{S_j}\boldsymbol{\mu}^{S_j} + \boldsymbol{\Psi}_{\mathrm{r}}^{S_j}\boldsymbol{\xi}_{\mathrm{r}}^{S_j} + \boldsymbol{\Psi}_{\mathrm{ar}}^{S_j}\boldsymbol{\xi}_{\mathrm{ar}}^{S_j}\\ &= (\boldsymbol{\Phi}^{S_j} - \boldsymbol{\Psi}_{\mathrm{ar}}^{\prime S_j\,\mathrm{a}}\boldsymbol{\Phi}^{S_j})\boldsymbol{\mu}^{S_j} + (\boldsymbol{\Psi}_{\mathrm{r}}^{S_j} - \boldsymbol{\Psi}_{\mathrm{ar}}^{\prime S_j\,\mathrm{a}}\boldsymbol{\Psi}_{\mathrm{r}}^{S_j})\boldsymbol{\xi}_{\mathrm{r}}^{S_j}\\ &\quad + \boldsymbol{\Psi}_{\mathrm{ar}}^{\prime S_j}\mathbf{x}_L^{S_j}\,, \end{aligned}\tag{16}$$

$$\mathbf{Q}^{S_j} = [\boldsymbol{\Phi}^{S_j} - \boldsymbol{\Psi}_{\mathrm{ar}}^{\prime S_j\,\mathrm{a}}\boldsymbol{\Phi}^{S_j}, \boldsymbol{\Psi}_{\mathrm{r}}^{S_j} - \boldsymbol{\Psi}_{\mathrm{ar}}^{\prime S_j\,\mathrm{a}}\boldsymbol{\Psi}_{\mathrm{r}}^{S_j}, \boldsymbol{\Psi}_{\mathrm{ar}}^{\prime S_j}], \tag{17}$$

where $\boldsymbol{\xi}_{\mathrm{ar}}^{S_j}$ are the generalized co-ordinates linked with the residual attachment modes. Concerning the hybrid interface methods with attachment modes, the same formulation gives :

$$\begin{aligned}\mathbf{x}^{S_j} &= \boldsymbol{\Phi}^{S_j}\boldsymbol{\mu}^{S_j} + \boldsymbol{\Psi}_{\mathrm{c}}^{S_j}\mathbf{x}_{L\mathrm{c}}^{S_j} + \boldsymbol{\Psi}_{\mathrm{a}}^{S_j}\boldsymbol{\xi}_{\mathrm{a}}^{S_j}\\ &= (\boldsymbol{\Phi}^{S_j} - \boldsymbol{\Psi}_{\mathrm{a}}^{\prime S_j\,\mathrm{a}}\boldsymbol{\Phi}^{S_j})\boldsymbol{\mu}^{S_j} + (\boldsymbol{\Psi}_{\mathrm{c}}^{S_j} - \boldsymbol{\Psi}_{\mathrm{a}}^{\prime S_j\,\mathrm{a}}\boldsymbol{\Psi}_{\mathrm{c}}^{S_j})\mathbf{x}_{L\mathrm{c}}^{S_j}\\ &\quad + \boldsymbol{\Psi}_{\mathrm{a}}^{\prime S_j}\mathbf{x}_{L\mathrm{a}}^{S_j}\,, \end{aligned}\tag{18}$$

$$\mathbf{Q}^{S_j} = [\boldsymbol{\Phi}^{S_j} - \boldsymbol{\Psi}_{\mathrm{a}}^{\prime S_j\,\mathrm{a}}\boldsymbol{\Phi}^{S_j}, \boldsymbol{\Psi}_{\mathrm{c}}^{S_j} - \boldsymbol{\Psi}_{\mathrm{a}}^{\prime S_j\,\mathrm{a}}\boldsymbol{\Psi}_{\mathrm{c}}^{S_j}, \boldsymbol{\Psi}_{\mathrm{a}}^{\prime S_j}], \tag{19}$$

and if we consider residual attachment modes, they become :

$$\begin{aligned}\mathbf{x}^{S_j} &= \boldsymbol{\Phi}^{S_j}\boldsymbol{\mu}^{S_j} + \boldsymbol{\Psi}_{\mathrm{c}}^{S_j}\mathbf{x}_{L\mathrm{c}}^{S_j} + \boldsymbol{\Psi}_{\mathrm{ar}}^{S_j}\boldsymbol{\xi}_{\mathrm{ar}}^{S_j}\\ &= (\boldsymbol{\Phi}^{S_j} - \boldsymbol{\Psi}_{\mathrm{ar}}^{\prime S_j\,\mathrm{a}}\boldsymbol{\Phi}^{S_j})\boldsymbol{\mu}^{S_j} + (\boldsymbol{\Psi}_{\mathrm{c}}^{S_j} - \boldsymbol{\Psi}_{\mathrm{ar}}^{\prime S_j\,\mathrm{a}}\boldsymbol{\Psi}_{\mathrm{c}}^{S_j})\mathbf{x}_{L\mathrm{c}}^{S_j}\\ &\quad + \boldsymbol{\Psi}_{\mathrm{ar}}^{\prime S_j}\mathbf{x}_{L\mathrm{a}}^{S_j}\,, \end{aligned}\tag{20}$$

$$\mathbf{Q}^{S_j} = [\boldsymbol{\Phi}^{S_j} - \boldsymbol{\Psi}_{\mathrm{ar}}^{\prime S_j\,\mathrm{a}}\boldsymbol{\Phi}^{S_j}, \boldsymbol{\Psi}_{\mathrm{c}}^{S_j} - \boldsymbol{\Psi}_{\mathrm{ar}}^{\prime S_j\,\mathrm{a}}\boldsymbol{\Psi}_{\mathrm{c}}^{S_j}, \boldsymbol{\Psi}_{\mathrm{ar}}^{\prime S_j}]. \tag{21}$$

CMS METHODS USING INTERFACE MODES

Classical component mode synthesis methods are time consuming in the case of large size problems, due to the interface co-ordinate vectors $\mathbf{x}_L^{S_j}$, $\mathbf{x}_{Lc}^{S_j}$ or $\mathbf{x}_{La}^{S_j}$ which could reach extensive sizes. Indeed, most of industrial models are made up of several sectors, containing themselves many hundred thousands degrees of freedom. Therefore, the idea consist in reducing the size of these vectors in each classical methods, by using the interface modes obtained after a static condensation [20] of the whole structure S on the interface L.

We denote by $\mathbf{\Psi}_C^S$, the n_L^S global constraint modes of S associated with the interface L. Thus, the constraint modes $\mathbf{\Psi}_C^{S_j}$ of the substructure S_j are the restriction to S_j of the vectors in $\mathbf{\Psi}_C^S$ associated with unit displacements imposed on the interface L^{S_j}. The interface modes $\mathbf{X}_L^S$ are definied as the l first eigenvectors of the reduced eigenproblem (22):

$$\mathbf{K}_L^S \mathbf{X}_L^S = \mathbf{M}_L^S \mathbf{X}_L^S \mathbf{\Omega}_L^2, \tag{22}$$

where $\mathbf{M}_L^S$ and $\mathbf{K}_L^S$ are the mass and stiffness reduced matrix obtained by projecting $\mathbf{M}^S$ and $\mathbf{K}^S$ on the global constraint modes $\mathbf{\Psi}_C^S$:

$$\mathbf{M}_L^S = {}^t\mathbf{\Psi}_C^S \mathbf{M}^S \mathbf{\Psi}_C^S \tag{23}$$

$$\mathbf{K}_L^S = {}^t\mathbf{\Psi}_C^S \mathbf{K}^S \mathbf{\Psi}_C^S. \tag{24}$$

The static lifting of $\mathbf{X}_L^S$ on the whole structure S leads to the global interface modes $\mathbf{\Phi}_L^S$, and their restriction to S_j, $\mathbf{\Phi}_L^{S_j}$ such as:

$$\mathbf{\Phi}_L^S = \mathbf{\Psi}_C^S \mathbf{X}_L^S \tag{25}$$

$$\mathbf{\Phi}_L^{S_j} = \mathbf{P}^{S_j} \mathbf{\Phi}_L^S. \tag{26}$$

As a matter of fact, the global interface modes $\mathbf{\Phi}_L^S$ represent the approximated vibration modes of the whole structure whose displacements are expressed as a linear combination of the global constraint modes $\mathbf{\Psi}_C^S$. As a consequence, the subspace generated by all the global interface modes ($\mathbf{\Phi}_L^S$ plus the non retained ones) is the same as the subspace generated by the global constraint modes $\mathbf{\Psi}_C^S$. As a consequence, since that the global interface modes have a real physical interpretation, the idea consists in replacing the global constraint modes $\mathbf{\Psi}_C^S$ by the l first global interface modes $\mathbf{\Phi}_L^S$.

In the fixed interface component mode synthesis methods, the displacements of S are expressed as:

$$\mathbf{x}^S = \mathbf{\Phi}^S \boldsymbol{\mu}_L + \mathbf{\Psi}_C^S \mathbf{x}_L^S, \tag{27}$$

where $\mathbf{\Phi}^S$ are the extensions to S of the substructure fixed interface normal modes $\mathbf{\Phi}^{S_j}$, and $\boldsymbol{\mu}^S$ is the vector containing all the substructure modal co-ordinates $\boldsymbol{\mu}^{S_j}$. As the global constraint modes $\mathbf{\Psi}_C^S$ span the same subspace than all the global interface modes, we can replace $\mathbf{\Psi}_C^S$ in the Ritz vectors $\mathbf{Q}^S = [\mathbf{\Phi}^S, \mathbf{\Psi}_C^S]$ by all the interface modes. The reduction procedure proposed by Bourquin [17,18] consists in performing a truncation of the interface modes, so that the global constraint modes $\mathbf{\Psi}_C^S$ are replaced by the l first global interface modes $\mathbf{\Phi}^S$. Thus, the displacements of S are written as:

$$\mathbf{x}^S = \mathbf{\Phi}^S \boldsymbol{\mu}^S + \mathbf{\Phi}_L^S \boldsymbol{\mu}_L, \tag{28}$$

where $\boldsymbol{\mu}_L$ is the vector of the generalized co-ordinates associated with $\mathbf{\Phi}_L^S$. This operation leads to a great reduction of the interface co-ordinates $\mathbf{x}_L^S$ because they are substituted by a small number l of generalized co-ordinates $\boldsymbol{\mu}_L$. Then, taking the restriction of Eqn. (27) to the substructures S_j, the expressions of the physical displacements $\mathbf{x}^{S_j}$ and the matrix of Ritz vectors $\mathbf{Q}^{S_j}$ become:

$$\mathbf{x}^{S_j} = \mathbf{\Phi}^{S_j} \boldsymbol{\mu}^{S_j} + \mathbf{\Phi}_L^{S_j} \boldsymbol{\mu}_L, \tag{29}$$

$$\mathbf{Q}^{S_j} = [\mathbf{\Phi}^{S_j}, \mathbf{\Phi}_L^{S_j}]. \tag{30}$$

In the cases of the free and hybrid interface component mode synthesis methods, the idea consists in introducing the expression of the constraint modes $\mathbf{\Psi}_C^{S_j}$ in the classical expressions the substructure displacements previously mentionned. As a result, they can be replaced by the interface modes with intention of reducing the size of the reduced systems. So, the expressions of physical displacements $\mathbf{x}^{S_j}$ and projection matrix are written as follows:

- free interface methods with attachment modes:

$$\mathbf{x}^{S_j} = (\mathbf{\Phi}^{S_j} - \mathbf{\Psi}_{\mathrm{ar}}^{\prime S_j\,\mathrm{a}} \mathbf{\Phi}^{S_j}) \boldsymbol{\mu}^{S_j} + (\mathbf{\Psi}_{\mathrm{r}}^{S_j} - \mathbf{\Psi}_{\mathrm{ar}}^{\prime S_j\,\mathrm{a}} \mathbf{\Psi}_{\mathrm{r}}^{S_j}) \boldsymbol{\xi}_{\mathrm{r}}^{S_j} + \mathbf{\Phi}_L^{S_j} \boldsymbol{\mu}_L; \tag{31}$$

$$\mathbf{Q}^{S_j} = [\mathbf{\Phi}^{S_j} - \mathbf{\Psi}_{\mathrm{ar}}^{\prime S_j\,\mathrm{a}} \mathbf{\Phi}^{S_j}, \mathbf{\Psi}_{\mathrm{r}}^{S_j} - \mathbf{\Psi}_{\mathrm{ar}}^{\prime S_j\,\mathrm{a}} \mathbf{\Psi}_{\mathrm{r}}^{S_j}, \mathbf{\Phi}_L^{S_j}]; \tag{32}$$

- free interface methods with residual attachment modes:

$$\mathbf{x}^{S_j} = (\mathbf{\Phi}^{S_j} - \mathbf{\Psi}_{\mathrm{ar}}^{\prime S_j\,\mathrm{a}} \mathbf{\Phi}^{S_j}) \boldsymbol{\mu}^{S_j} + (\mathbf{\Psi}_{\mathrm{r}}^{S_j} - \mathbf{\Psi}_{\mathrm{ar}}^{\prime S_j\,\mathrm{a}} \mathbf{\Psi}_{\mathrm{r}}^{S_j}) \boldsymbol{\xi}_{\mathrm{r}}^{S_j} + \mathbf{\Phi}_L^{S_j} \boldsymbol{\mu}_L; \tag{33}$$

$$\mathbf{Q}^{S_j} = [\mathbf{\Phi}^{S_j} - \mathbf{\Psi}_{\mathrm{ar}}^{\prime S_j\,\mathrm{a}} \mathbf{\Phi}^{S_j}, \mathbf{\Psi}_{\mathrm{r}}^{S_j} - \mathbf{\Psi}_{\mathrm{ar}}^{\prime S_j\,\mathrm{a}} \mathbf{\Psi}_{\mathrm{r}}^{S_j}, \mathbf{\Phi}_L^{S_j}]; \tag{34}$$

- hybrid interface methods with attachment modes :

$$\mathbf{x}^{S_j} = (\mathbf{\Phi}^{S_j} - \mathbf{\Psi}_{\mathrm{a}}^{\prime S_j\,\mathrm{a}}\mathbf{\Phi}^{S_j})\boldsymbol{\mu}^{S_j} + \mathbf{\Phi}_L^{S_j}\boldsymbol{\mu}_L\,; \tag{35}$$

$$\mathbf{Q}^{S_j} = [\mathbf{\Phi}^{S_j} - \mathbf{\Psi}_{\mathrm{a}}^{\prime S_j\,\mathrm{a}}\mathbf{\Phi}^{S_j}\,, \mathbf{\Phi}_L^{S_j}]\,; \tag{36}$$

- hybrid interface methods with residual attachment modes :

$$\mathbf{x}^{S_j} = (\mathbf{\Phi}^{S_j} - \mathbf{\Psi}_{\mathrm{ar}}^{\prime S_j\,\mathrm{a}}\mathbf{\Phi}^{S_j})\boldsymbol{\mu}^{S_j} + \mathbf{\Phi}_L^{S_j}\boldsymbol{\mu}_L\,; \tag{37}$$

$$\mathbf{Q}^{S_j} = [\mathbf{\Phi}^{S_j} - \mathbf{\Psi}_{\mathrm{ar}}^{\prime S_j\,\mathrm{a}}\mathbf{\Phi}^{S_j}\,, \mathbf{\Phi}_L^{S_j}]\,. \tag{38}$$

These different formulations allow to reduce significantly the projected system (9). The number l of generalized co-ordinates $\boldsymbol{\mu}_L$ depends on the precision required or on a user choice (typically defined by a criterion like the Rubin criterion), whereas the size of displacements vector $\mathbf{x}_L^{S_j}$ is necessarily the same as the number of degrees of freedom at the interface L.

PROCEDURE

The following scheme represents the calculation chain we have to implement in order to predict the forced response of rotating mistuned bladed disks based on a component mode synthesis approach with interface modes. The objective is to develop an accurate and efficient reduction procedure of finite element models. This algorithm consists in the main following steps :

1. Computation of normal modes (with fixed, free or hybrid interface) and static modes (constraint, attachment or residual attachment modes) of D_j and B_j, for $j = 0, ..., N-1$;
2. Computation of the interface modes $\mathbf{\Phi}_L^{D_j}$ and $\mathbf{\Phi}_L^{B_j}$: computation of $\mathbf{M}_L^S$, $\mathbf{K}_L^S$, and the interface modes $\mathbf{X}_L^S$, Eqn. (22), then static lifting to obtain $\mathbf{\Phi}_L^S$, and extraction of $\mathbf{\Phi}_L^{D_j}$ and $\mathbf{\Phi}_L^{B_j}$. In practice, $\mathbf{M}_L^S$ and $\mathbf{K}_L^S$ are obtained by assembling reduced mass and stiffness matrices of D_j and B_j, which result from the static condensation of D_j to L^{D_j}, and B_j to L^{B_j} ;
3. Computation of the Ritz vectors $\mathbf{Q}^{S_j} = [\mathbf{Q}'^{S_j}, \mathbf{\Phi}_L^{S_j}]$, for $j = 0, ..., N-1$, from the normal, static and interface modes previously obtained, and where $\mathbf{Q}'^{S_j}$ are the vectors of $\mathbf{Q}^{S_j}$ defined in Eqns. (30), (32), (34), (36) and (38) ;
4. Projection of disk matrices $\mathbf{K}_{\mathrm{tuned}}^{D_j} + \Delta\mathbf{K}^{D_j}$ and external forces $\mathbf{f}^{D_j}$ on $\mathbf{Q}^{D_j} = [\mathbf{Q}'^{D_j}, \mathbf{\Phi}_L^{D_j}]$, with $\Delta\mathbf{K}^{D_j} = 0$ if the disk is tuned :

$$\mathbf{K}_{\mathrm{r}}^{D_j} = {}^t\mathbf{Q}^{D_j}\mathbf{K}_{\mathrm{tuned}}^{D_j}\mathbf{Q}^{D_j} + {}^t\mathbf{Q}^{D_j}\Delta\mathbf{K}^{D_j}\mathbf{Q}^{D_j}\,, \tag{39}$$

$$\mathbf{f}_{\mathrm{r}}^{D_j} = {}^t\mathbf{Q}^{D_j}\mathbf{f}^{D_j}\,. \tag{40}$$

Same projections for $\mathbf{M}^{D_j}$ and $\mathbf{B}^{D_j}$.

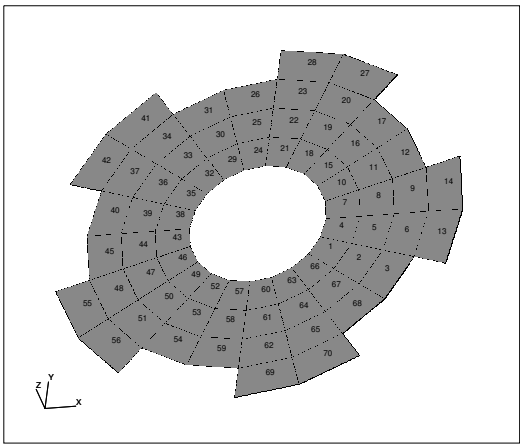

Figure 2. STRUCTURAL MESH OF THE BLADED DISK.

5. Projection of the mistuned blade matrices $\mathbf{K}_{\mathrm{tuned}}^{B_j} + \Delta\mathbf{K}^{B_j}$ and external forces $\mathbf{f}^{B_j}$ on $\mathbf{Q}^{B_j} = [\mathbf{Q}'^{B_j}, \mathbf{\Phi}_L^{B_j}]$:

$$\mathbf{K}_{\mathrm{r}}^{B_j} = {}^t\mathbf{Q}^{B_j}\mathbf{K}_{\mathrm{tuned}}^{B_j}\mathbf{Q}^{B_j} + {}^t\mathbf{Q}^{B_j}\Delta\mathbf{K}^{B_j}\mathbf{Q}^{B_j}\,, \tag{41}$$

$$\mathbf{f}_{\mathrm{r}}^{B_j} = {}^t\mathbf{Q}^{B_j}\mathbf{f}^{B_j}\,. \tag{42}$$

Same projections for $\mathbf{M}^{B_j}$ and $\mathbf{B}^{B_j}$.

6. Assembly of the reduced matrices $\mathbf{K}_{\mathrm{r}}^{D_j}$, $\mathbf{K}_{\mathrm{r}}^{B_j}$, $\mathbf{M}_{\mathrm{r}}^{D_j}$, $\mathbf{M}_{\mathrm{r}}^{B_j}$, $\mathbf{B}_{\mathrm{r}}^{D_j}$, $\mathbf{B}_{\mathrm{r}}^{B_j}$, and vectors of exrnal forces $\mathbf{f}_{\mathrm{r}}^{D_j}$ and $\mathbf{f}_{\mathrm{r}}^{B_j}$, for $j = 0, ..., N-1$, thought the interface co-ordinates to obtain reduced assemblied matrices $\mathbf{K}_{\mathrm{r}}^S$, $\mathbf{M}_{\mathrm{r}}^S$, $\mathbf{B}_{\mathrm{r}}^S$, and generalized forces $\mathbf{f}_{\mathrm{r}}^S$;
7. Resolution of the following problem :

$$\mathbf{M}_{\mathrm{r}}^S\ddot{\mathbf{q}}^{S_j} + \mathbf{B}_{\mathrm{r}}^S\dot{\mathbf{q}}^{S_j} + \mathbf{K}_{\mathrm{r}}^S\mathbf{q}^{S_j} = \mathbf{f}_{\mathrm{r}}^S\,; \tag{43}$$

8. Finally, extraction of $\mathbf{q}^{S_j}$ from $\mathbf{q}^S$, then computation of the physical displacements of S_j with $\mathbf{x}^{S_j} = \mathbf{Q}^{S_j}\mathbf{q}^{S_j}$ and determination of $\mathbf{x}^S$ by assembing $\mathbf{x}^{S_j}$ for $j = 0, ..., N-1$.

APPLICATIONS

A simplified development model (Fig. 2) with five blades was used to program and validate the classical CMS methods, and those using interface modes, taking into account, or not, the different terms generated by the rotation.

The structural finite element mesh of the complete bladed disk has 375 degrees of freedom (5 per node). It is made up of 70 elements QUAD4 and the reference sector has only 14 elements. The inner, outer, and overall outer radius of the disk are respectively $40 \times 10^{-3}\,m$, $100 \times 10^{-3}\,m$ and $120 \times 10^{-3}\,m$, the thickness

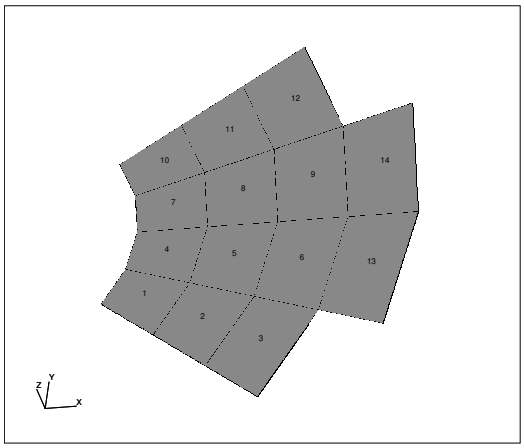

Figure 3. STRUCTURAL MESH OF THE REFERENCE SECTOR.

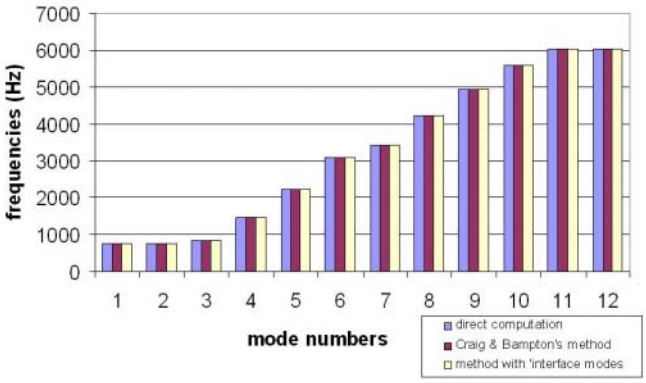

Figure 5. COMPARISON OF THE DIFFERENT FIXED INTERFACE CMS METHODS.

of the plate is $5 \times 10^{-3} m$. Young's modulus , Poisson's ratio and density of the bladed disk are respectively $2.11 \times 10^{11} N/m^2$, 0.3, and $7860 kg/m^3$.

In fact, only one reference sector (Fig. 3) which is composed by two sub-structures, is modelized and used to compute mass, elastic stiffness, rotational matrices, and also static modes for the projections.

Effects due to the rotational terms

A study of effects caused by the different matrices generated by the rotation on vibrational frequencies has been realized on the tuned model (Fig. 4).

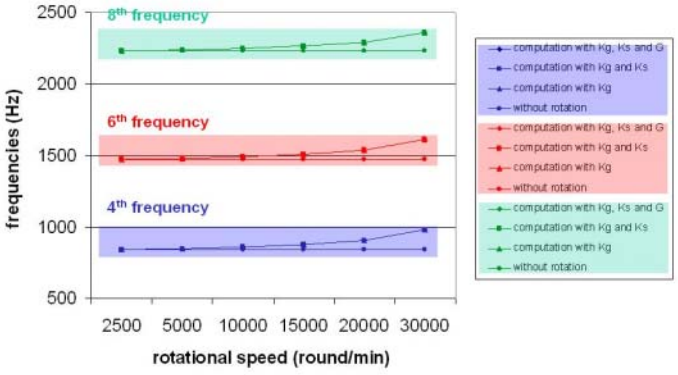

Figure 4. EFFECTS ON FREQUENCIES DUE TO THE ROTATIONAL TERMS.

This study show that the centrigal stress stiffning effet provided by matrix $\mathbf{K}_{\mathrm{G}}^{S}$ is preponderant compared to the softening effect due to matrix $\mathbf{K}_{\mathrm{S}}^{S}$ and the gyroscopic effect provided b $\mathbf{G}^{S}$. Ideed, the Campbel diagrams are practically the sames for computations with $\mathbf{K}_{\mathrm{G}}^{S}$ only, $\mathbf{K}_{\mathrm{G}}^{S} + \mathbf{K}_{\mathrm{S}}^{S}$, and $\mathbf{K}_{\mathrm{G}}^{S} + \mathbf{K}_{\mathrm{S}}^{S}$ and $\mathbf{G}^{S}$, as represented on Fig. 4 for the 4^{th}, 6^{th}, and 8^{th} vibrational frequencies.

Comparison of fixed interface CMS methods

Classical CMS methods and CMS methods with interface modes have been implemented in the case of fixed interfaces. They have been evaluated on the tuned model in rotation presented previously, and results have been compared to a reference solution provided by a direct computation in a FE code (NASTRAN).

Fig. 5 shows that the twelves first vibrational frequencies are in a good agreement between the reference solution, the classical CMS method (maximum error $= 8 \times 10^{-3}\,\%$) with 150 interface co-ordinates, and the CMS method using interface modes (maximum error $= 6.1 \times 10^{-1}\,\%$) with only 20 interface co-ordinates. These results are obtained from the rotating reference sector ($5000 tr/min$), with matrices $\mathbf{K}_{\mathrm{G}}^{S}$ and $\mathbf{K}_{\mathrm{S}}^{S}$, using 10 normal modes for the part of disk and 4 for the blade.

CONCLUSION

Methods based on the use of the interface modes were presented in order to predict the forced response of rotating mistuned bladed disks. In these methods, the static modes are replaced by the interface modes, which result from a static condensation of the entire structure on the whole interface. This approach has already been applied in case of tuned bladed disks in combination with cyclic symmetry, and its application to mis-

tuned bladed disks is in progress as a part of a doctoral dissertation. Adaptations and a resolution scheme have been explained, taking into account that all sectors might be mistuned. Numerical simulations are currently carried out to demonstrate the efficiency of the proposed approach. Eigensolutions obtained on a rotating development model with classical methods and methods with interface modes have been compared, and have shown a good agreement with a reference solution. Future work will consist in taking aerodynamics into account, using an indirect fluid-structure coupling formulation.

REFERENCES

[1] Pierre, C., and Murthy, D. V., 1992. "Aeroelastic modal characteristics of mistuned blade assemblies : Mode localization and loss of eigenstructure". *AIAA Journal,* **30**(10), Oct., pp. 2483–2496.

[2] Kruse, M. J., and Pierre, C., 1997. "An experimental investigation of vibration localization in bladed disks. Part I : Free response". In ASME Paper 97-GT-501 Proceedings of the ASME Gas Turbine Conference, Orlando, Florida.

[3] Kruse, M. J., and Pierre, C., 1997. "An experimental investigation of vibration localization in bladed disks Part II : Forced response". In ASME Paper 97-GT-501 Proceedings of the ASME Gas Turbine Conference, Orlando, Florida.

[4] Kaza, K. R. V., and Kielb, R. E., 1982. "Flutter and response of a mistuned cascade in incompressible flow". *AIAA Journal,* **20**, pp. 1120–1127.

[5] Kaza, K. R. V., and Kielb, R. E., 1984. "Flutter of turbofan rotors with mistuned blades". *AIAA Journal,* **22**(11), Nov., pp. 1618–1625.

[6] Yang, M.-T., and Griffin, J. H., 2001. "A reduced-order model of mistuning using a subset of nominal system modes". *ASME Journal of Engineering for Gas Turbines and Power,* **123**(4), Oct., pp. 893–900.

[7] Moyroud, F., Fransson, T., and Jacquet-Richardet, G., 2002. "A comparison of two finite element reduction techniques for mistuned bladed disks". *ASME Journal of Engineering for Gas Turbines and Power,* **124**(4), Oct., pp. 942–952.

[8] Bladh, R., Castanier, M. P., and Pierre, C., 2001. "Component-mode-based reduced order modeling techniques for mistuned bladed disks. Part I : Theoretical models". *ASME Journal of Engineering for Gas Turbines and Power,* **123**(1), Jan., pp. 89–99.

[9] Hurty, W. C., 1965. "Dynamic analysis of structural systems using component modes". *AIAA Journal,* **3**(4), Apr., pp. 678–685.

[10] Craig, Jr., R. R., and Bampton, M. C. C., 1968. "Coupling of substructures for dynamic analysis". *AIAA Journal,* **6**(7), July, pp. 1313–1319.

[11] Goldman, R. L., 1969. "Vibration analysis by dynamic partitioning". *AIAA Journal,* **7**(6), pp. 1152–1154.

[12] Rubin, S., 1975. "Improved component-mode representation for structural dynamic analysis". *AIAA Journal,* **13**(8), Aug., pp. 995–1006.

[13] MacNeal, R. H., 1971. "A hybrid method of component mode synthesis". *Computers & Structures,* **1**(4), pp. 581–601.

[14] Benfield, W. A., and Hruda, R. F., 1971. "Vibration analysis of structures by component mode substitution". *AIAA Journal,* **9**(7), July, pp. 1255–1261.

[15] Henry, R., 1981. "Contribution à l'étude dynamique des machines tournantes". PhD thesis, Institut National des Sciences Appliquées de Lyon.

[16] Valid, R., and Ohayon, R., 1985. "Théorie et calcul statique et dynamique des structures à symétries cycliques". *LRA*(4), July-Aug., pp. 251–263.

[17] Bourquin, F., 1991. "Synthèse modale et analyse numérique des mulitistructures élastiques". PhD thesis, Université Pierre et Marie, Paris 6.

[18] Bourquin, F., 1992. "Component mode synthesis and eigenvalues of second order operators : Discretization and algorithm". *Modelisation Mathématique et Analyse Numérique,* **44**(1-2), pp. 385–423.

[19] Tran, D.-M., 2001. "Component mode synthesis methods using interface modes. Application to structures with cyclic symmetry". *Computers & Structures,* **79**(1), pp. 209–222.

[20] Guyan, R. J., 1965. "Reduction of stiffness and mass matrices". *AIAA Journal,* **3**(2), May, pp. 960–961.